Laboratory study on the behaviour of spent AA household alkaline batteries in incineration

Manuel F. Almeida *, Susana M. Xará, Julanda Delgado, Carlos A. Costa

ABSTRACT

The quantitative evaluation of emissions from incineration is essential when Life Cycle Assessment (LCA) studies consider this process as an end-of-life solution for some wastes. Thus, the objective of this work is to quantify the main gaseous emissions produced when spent AA alkaline batteries are incinerated. With this aim, batteries were kept for 1 h at 1273 K in a refractory steel tube hold in a horizontal electric furnace with temperature control. At one end of the refractory steel tube, a constant air flow input assures the presence of oxygen in the atmosphere and guides the gaseous emissions to a filter system followed by a set of two bubbler flasks having an aqueous solution of 10% (v/v) nitric acid. After each set of experiments, sulphur, chlorides and metals (As, Cd, Co, Cr, Cu, Fe, Hg, Mn, Ni, Pb, Sb, Tl and Zn) were analyzed in both the solutions obtained from the steel tube washing and from the bubblers. Sulphur, chlorides and metals were quantified, respectively, using barium sulfate gravimetry, the Volhard method and atomic absorption spectrometry (AAS).

The emissions of zinc, the most emitted metal, represent about 6.5% of the zinc content in the batteries. Emissions of manganese (whose oxide is the main component of the cathode) and iron (from the cathode collector) are negligible when compared with their amount in AA alkaline batteries. Mercury is the metal with higher volatility in the composition of the batteries and was collected even in the second bubbler flask. The amount of chlorides collected corresponds to about 36% of the chlorine in the battery sleeve that is made from PVC. A considerable part of the HCl formed in PVC plastic sleeve incineration is neutralized with KOH, zinc and manganese oxides and, thus, it is not totally released in the gas.

Some of the emissions are predictable through a thermodynamic data analysis at temperatures in the range of 1200–1300 K taking into account the composition of the batteries. This analysis was done for most of potential reactions between components in the batteries as well as between them and the surrounding atmosphere and it reasonably agrees the experimental results.

The results obtained show the role of alkaline batteries at the acid gases cleaning process, through the neutralization reactions of some of their components. Therefore, LCA of spent AA alkaline batteries at the municipal solid waste (MSW) incineration process must consider this contribution.

1. Introduction

LCA methodology may be used to support either small domestic spent batteries flow management options or MSW disposal alternatives where batteries are present. High temperature processes, for example, loading spent batteries in iron blast furnaces and MSW incineration, are argued as good practices for managing this type of wastes. The lack of data on this subject and the need to follow a LCA approach is recognized even for the development of new legislation (Labouze and Monier, 2003).

With the objective of assessing the environmental impact resulting from incineration of spent AA alkaline batteries, this process was simulated on a laboratory scale. The tests took place in a tubular oven where batteries were heated in air and off-gases collected for emissions quantification, thus seeking confident results to fulfill the lack of data on the behavior of batteries in incineration processes. Previously to this work, a chemical and physical characterization of the target batteries was made, in order to provide up-to-date information about this waste stream. These results were presented in a previous paper, and they may help in understanding some of the transformations that occur during the incineration process (Almeida et al., 2006).

The previous results indicated that spent AA alkaline Duracell® batteries have an average weight of 23.5 g, of which 8.5% is moisture content. The most meaningful components are a cathode, with MnO_2, graphite and potassium hydroxide, a nickel-plated steel can as cathode collector, and an anode containing zinc, zinc oxide and potassium hydroxide as electrolyte. Other components in the batteries are: one separator and one cap (both in steel), a tin-plated brass as anode collector, a PVC plastic sleeve, a polyamide grommet, a cardboard insulator, and a paper and a cellophane separator (Almeida et al., 2006).

An incineration plant is operated in such a way that the gas resulting from the process is raised, after the last injection of combustion air, in a controlled and homogeneous fashion and even under the most unfavorable conditions, to a temperature of at least 1123 K (European Parliament and Council, Directive 2000/76/EC, 2000). Thus, the incinerator furnace temperature for MSW is generally above 1150 K, most of the time in the range of 1200–1300 K. When batteries are loaded into such a furnace, they inevitably suffer some deep transformations. One of the most expected changes comes from the 2 g of moisture contained in the batteries that is suddenly transformed into 2500 ml of steam. Consequently, batteries explode, thus exposing the internal components to the furnace oxidant atmosphere, since on average incinerators operate with an overstoichiometric amount of air.

Some of the changes in batteries may be anticipated through the oxidation reactions as shown in Table A.1 (Appendix) and may explain part of the emissions during the MSW incineration process. Other emissions come from the chloridizing reactions between HCl, formed by combustion of PVC sleeve, and some metals and oxides present in the batteries, as seen in Table A.2 (Appendix).

2. Experimental

The laboratory system used to simulate the incineration of batteries is depicted in Fig. 1. It includes an electric furnace, with temperature control, holding a Cr–Ni refractory steel tube of 54 mm internal diameter. At one end of the tube a constant air flow input of 200 N ml min^{-1} assures the presence of oxygen inside and guides the generated emissions to the other end of the tube. There, a filter of 0.7 μm pore size is placed just before the polymeric tube connection for two sequential bubbler flasks. These flasks are filled with 100 ml of 10% (v/v) HNO_3 aqueous solution where bubbling gas is dispersed through sintered ceramic disks. Five experiments of 10 batteries each were performed. Each battery was kept inside the furnace at 1273 K for 1 h. A blank test with no batteries was carried out at the same temperature, holding the refractory steel tube for 10 h. The off-gases were cleaned exactly in the same way through the system and the solutions obtained were analyzed as described below for the tests with batteries.

Prior to loading batteries into the furnace, they were cross-cut into two pieces at the middle lengthwise and placed in an open kaolin container in order to avoid the contact with the internal wall of the refractory steel tube. This procedure also prevents contamination of the internal steel tube walls by the potential projections resulting from any explosion, since steam from moisture can be smoothly released through the two open cross-cut extremities of the battery. Furthermore, using a fixed length container that is pushed always at the same distance through the tube assures that all batteries take the same position inside the furnace.

Each experiment started with heating the furnace up to 1273 K. Once at this temperature, the input air end of the tube was screwed-off and the container with the two cross-cut pieces of the battery was pushed inside the tube to the middle length of the furnace. A few seconds later the top of the tube was screwed-on, the air input turned on and the off-gases start flowing through the collection system, i.e., the filter and the two sequential bubbler flasks. After keeping the battery at 1273 K for 1 h, the furnace was cooled to ambient temperature, the air flow was off and the container with battery carefully removed. The procedure was then repeated for the other batteries of the experiment (total of 10 batteries). At the end of each experiment, the refractory steel tube was taken off and 200 ml of fresh 10% (v/v) HNO_3 aqueous solution was used to methodically wash both its inner walls and the filter. The solution from each bubbler flask was added to 50 ml of fresh 10% (v/v) HNO_3 aqueous solution used to wash the flask and the connection tube. The emissions of each experiment of 10 batteries were thus collected in 3 aqueous solutions of 10% (v/v) HNO_3: (i) 200 ml from washing the inner walls of the refractory steel tube and the filter; (ii) 150 ml obtained by adding 100 ml from the first gas washing flask with 50 ml of solution used to wash the flask and the piece of tube between it and the filter; and (iii) 150 ml obtained with the 100 ml of solution in the second flask and the 50 ml of solution from washing the flask and the piece of tube between flasks. These three solutions with volumes of 200, 150 and 150 ml were named Furn, Fk1 and Fk2, respectively.

The sulfur content in these solutions was determined as sulfate using a gravimetric method (American Public Health Association, 1992). Chlorides were quantified using the Volhard method (Bassett et al., 1981). Cd, Co, Cr, Cu, Mn, Fe, Ni, Pb, Sb, Tl and Zn were quantified by AAS using the direct aspiration method (USEPA, 1982). Hg and As were also quantified by AAS, using, respectively, the cold vapor generation and the hydride generator techniques (USEPA, 1982). The amount of each element was calculated through the respective solution concentration and volume, corrected for the values of the blank test. When the element in the solution was below the detection limit of the method of analysis, its concentration was taken as the mean value of the interval [0-detection limit].

3. Results and discussion

Table 1 shows the values corresponding to the blank test. Despite the furnace tube material being refractory steel with high content in Fe, Cr and Ni, and 0.05% Cu, 0.1% Mn, only negligible amounts of all these metals were found in Furn solution. Most of the values in Table 1 are the average between zero and the detection limit of the respective element, therefore not detected. Table 2 shows emissions per kg of batteries for the five sets of experiments, the respective mean values and ranges. These values were already corrected for those shown in Table 1. Fig. 2 presents the emissions distribution in the experimental off-gas collection system.

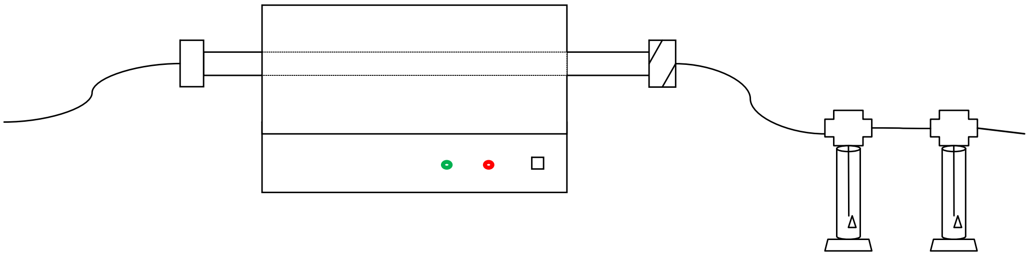

Fig. 1. Laboratorial test set-up to simulate incineration of the alkaline batteries – tubular furnace and bubblers flasks.

Table 1
Emissions from blank test performed during 10 h at 1273 K (in mg; As and Hg, in μg)

Emission	Furn	Fk1	Fk2
SO_4^{2-}	*0.75*	*0.75*	*0.75*
Cl	*0.68*	*0.68*	*0.68*
As	1.29	*0.03*	*0.03*
Cd	*0.00*	*0.00*	*0.00*
Co	0.01	*0.01*	*0.01*
Cr	0.18	*0.00*	*0.00*
Cu	0.01	*0.00*	*0.00*
Fe	0.50	*0.00*	*0.00*
Hg	0.45	0.50	0.26
Mn	0.09	*0.00*	*0.00*
Ni	*0.00*	*0.00*	*0.00*
Pb	0.03	*0.01*	*0.01*
Sb	*0.03*	*0.03*	*0.03*
Tl	*0.02*	*0.02*	*0.02*
Zn	1.11	0.03	0.01

The italicised values correspond to solutions where the amount determined was below the detection limit of the quantification method used (for computation purpose the concentration considered was half of the detection limit).

Table 2
Emissions from alkaline AA Duracell® batteries (mg kg^{-1} of batteries, except As and Hg expressed in μg kg^{-1})

Emission	Exp 1	Exp 2	Exp 3	Exp 4	Exp 5	Mean	Range
SO_4^{2-}	47.9	7.9	39.6	19.1	28.7	28.6	7.9–47.9
Cl	1714	2180	1920	2239	1743	1959	1714–2239
As	N.D.	0.08	0.64	2.12	N.D.	0.57	N.D.–2.12
Cd	0.26	0.19	0.19	0.36	0.30	0.26	0.19–0.36
Co	1.44	0.15	0.20	0.11	0.05	0.39	0.05–1.44
Cr	34	119	299	32	32	103	32–299
Cu	1.63	1.54	5.10	4.21	7.06	3.91	1.54–7.06
Fe	1795	92	96	135	60	436	60–1795
Hg	16.85	23.78	1.47	N.D.	2.55	8.93	N.D.–23.78
Mn	315	21	21	12	37	81	12–315
Ni	8.91	0.45	0.50	0.87	0.43	2.23	0.43–8.91
Pb	16.67	12.46	7.86	24.16	14.99	15.23	7.86–24.16
Sb	0.27	0.08	N.D.	N.D.	N.D.	0.07	N.D.–0.27
Tl	0.67	0.61	0.47	0.34	0.11	0.44	0.11–0.67
Zn	17082	10440	8794	6130	5387	9567	5387–17082

N.D., not detectable.

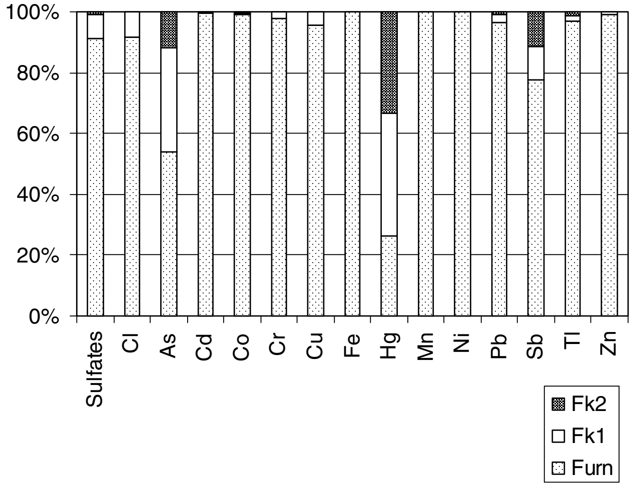

Fig. 2. Distribution of five experiments average emissions in the three washing solutions of the experimental off-gas collecting system, respectively furnace (Furn), first bubbler flask (Fk1) and second bubbler flask (Fk2).

As seen, most of the emissions were collected at the refractory steel tube whose off-gases outlet extremity remained always below 420 K. The significant exception is mercury, most of which is collected at the first washing flask and a smaller amount at the second flask. This is not unexpected, since this metal boils at 629 K, and has significant vapor pressure at temperatures below 420 K. Hg(II) chloride has still higher volatility than the metal, therefore, once produced through reaction 64 (see in Appendix) near batteries, it can be transported far away from the 1273 K hot zone along the cleaning system. Mercury emitted and collected corresponds only to about 5.3% of the battery content.

Fig. 2 depicts relatively high emissions for Sb and Tl collected at the two washing flasks. This is because of the assumption that their concentration in the solutions is the middle of range between zero and the respective detection limit. In fact, the total emission is small if compared to the analytical method sensitivity limit. These two elements are present as traces, mainly at the batteries cathode and cathode collector, and have a reasonable vapor pressure at 1200–1300 K either as chlorides, oxides or metals whose formation is demonstrated possible according reactions 22–24 and 58–61 in Tables A.1 and A.2.

Chlorides are important emissions in the combustion of batteries. Most of HCl results from PVC sleeve combustion (see Eq. (1) in Appendix), and, being a gas at ambient temperature, it should be collected outside of the refractory steel tube. However, experimental results show that most of chlorides condensate at the tube walls and at the filter, that indicating lower volatility than HCl. Therefore, some of these chlorides are not HCl but are volatile salts that result from reaction of HCl with other components in the batteries. Some of the possible chloridizing reactions shown in Table A.2 are those having negative ΔG°, i.e., reactions 30–34, 36–39, 42, 43, 47, 49–53, 56–62, 64, and 65. Reactions 32, 36 and 49 require a reducing atmosphere to occur, which may happen in relatively short periods of time during the laboratory incineration process because of the constant air flow through the steel tube (in an MSW incinerator it may happen for short periods and in limited areas taking into account that in average incinerators operate with an overstoichiometric amount of air). Other reactions, despite $\Delta G^\circ < 0$, are practically unfeasible due to the lack or scarcity of one of the reactants, for example, reaction 42 that requires improbable chromium (VI) oxide as reactant. Possible, but very improbable, are the reactions with $\Delta G^\circ > 0$ unless integrated in an overall chain of reactions with $\Delta G^\circ < 0$. Therefore, the chloridizing reactions that better explain chlorides that condensate at the refractory steel tube walls and at the filter are those involving HCl and the most abundant components in batteries, namely Zn, ZnO, Mn_3O_4, Fe, KOH and Cu (from tin-plated brass anode collector). However, KCl is the less volatile of those possible resulting chlorides and it has no significant vapor pressure at the temperatures tested. The mean value for the chlorides collected at the off-gas cleaning system is 1.96 g kg^{-1} of batteries, which corresponds to 36.4% of the chlorine present in the PVC sleeve (assuming that PVC contains about 55% Cl). Therefore, most of the HCl generated at the combustion process of the PVC sleeve seems to be neutralized and retained by reactions with components present in the batteries there remaining as metallic chlorides, mainly with KOH of the electrolyte through reaction 65 (Table A.2).

Zinc is the metal most emitted by burned batteries. Despite the important amount emitted (about 9.6 g per kg of batteries), it represents only about 6.5% of the zinc contained in the batteries. Most of it comes from unspent metallic zinc on the anode that is vaporized at 1179 K, further oxidized according to reaction 1 (Table A.1). ZnO condensates on the inner walls of the refractory steel tube and some particles may be transported up to the filter, as shown by the respective bar in Fig. 2. However, due to reactions 30 and 31, some of it may be released as zinc chloride, perhaps the small amount of zinc that is found in the first washing flask, since zinc chloride is more volatile than zinc.

Iron was practically all collected at the refractory tube at levels significantly higher than in the blank test. Most probably, values emitted are the result of reactions 33, 34 and 36, between HCl from PVC sleeve combustion and iron from the cathode collector protected by the sleeve, therefore both reactants very close of each other. Outside steel can shows high potential of reaction, mostly through reaction 9 (Table A.1), as demonstrated by an experiment carried out where a 42.5% weight increase was observed when this material was held for 1 h at 1273 K in atmospheric air. Although in less favorable conditions, through reactions 33, 34 and 36 (Table A.2), iron at the refractory steel tube may react with HCl released from PVC combustion, too. In this case some of the values found in the Furn solution may not totally correspond to iron emissions from batteries.

Although Fig. 2 shows some traces of nickel collected in the two washing flasks Fk1 and Fk2, these small amounts are a consequence of the computation method that still considers its presence when in concentration below the detection limit in both the solutions. Nevertheless, as seen in Fig. 2, it was found in detectable levels in the refractory tube, contrary to the blank test observations. Perhaps, it is a consequence of reaction 37, between HCl resulting from PVC sleeve combustion and nickel coating from the nickel-plated steel cathode collector. As the refractory steel tube has a very high percentage of Ni, an interaction between it and the HCl from the sleeve combustion could also be considered, in this case generating false emissions from batteries.

Most of the chromium emissions are found at the steel tube at levels significantly higher than at the blank test as indicated by Fig. 2. Furthermore, all the tests with batteries indicate transport of a small amount of chromium to the first washing flask. Therefore, the cause for these emissions must be found in the composition of the batteries. Eqs. (16) and (18) (Table A.1) and the volatility of the respective formed oxides may offer some explanation to that fact. KOH from electrolyte has vapor pressure of about 2.6–8.3 kPa in the range of 1200–1300 K, that makes the released caustic vapor able to contact with chromium bearing components of the batteries and that in the refractory steel tube. Chromium in contact with oxygen is known to be predominantly oxidized to Cr_2O_3 through reaction 15. This chromium sesquioxide may react with KOH through Eq. (27), giving potassium chromate. As this salt is very soluble in water, when the inner wall of the refractory tube is washed, it brings chromium into the washing solution at levels higher than in the blank test. Therefore, it is probable that most of chromium found in the washing steel tube solution results from its reaction with KOH vapor and not from any reaction with chromium bearing components of batteries.

Manganese is almost all collected inside the refractory tube at levels significantly higher than at the blank test. However, these values are insignificant when compared to the manganese content in the batteries. Since both manganese and its oxides do not volatilize appreciably at 1273 K, the probable cause for the values reported as emissions is the manganese chloride resulting from reaction 32, between HCl from sleeve combustion and manganese oxide present in the cathode. Non-perceptible projections from the cathode to the refractory steel tube walls could justify false manganese emissions, too.

On average, lead emissions represent about 1.27% of total lead in the batteries, corresponding to approximately 57.5% of its content on the PVC sleeve. Reaction 50, between the two reagents both present in the PVC plastic sleeve, releases volatile $PbCl_2$ that may explain its partial transport to the first washing flask.

Copper is the main element on the anode collector practically representing all existing copper in the batteries and shares 8.6% of all metal components on them (Almeida et al., 2006). The amount of copper released is comparatively insignificant and a small fraction of it is washed out at the first flask. Reactions 43 and 44, between HCl from the PVC sleeve and copper on the anode collector may explain its presence in the off-gases and its origin in the batteries.

Cadmium may be released due to its high volatility as metal as well as a result of reactions 56 and 57. The emissions of cadmium correspond to about 10.2% of the total estimated as present in AA alkaline batteries.

Approximately, 1.1% of cobalt in batteries is released as chlorides, probably due to reactions 52 and 53.

Arsenium may be released as element, oxide or chloride, according to reactions 21 and 22. These emissions correspond only to 0.05% of the element content found as trace in batteries.

Soluble sulfur present in batteries is reported as sulfates. It was mainly detected at the cathode composition and it only represents about 0.37% of its total weight. Sulfur in other components was not analyzed in the characterization work (Almeida et al., 2006). Thus, the sulfur emissions here computed cannot be compared with its content in the batteries. Anyway, these values are significant, and, probably, may correspond to sulfur released during the cathode coal combustion or some other combustible fraction, for example, paper components. In fact, sulfur originated from sulfates is improbable due to the fact that most of the sulfates are stable and do not decompose significantly at temperatures below 1273 K. Any hypothetic unstable sulfate salt present at either the anode or cathode would be decomposed in SO_3 and its oxide counterpart, and, following, its sulfur stabilized with KOH from impregnated electrolyte through reaction 29, in the form of K_2SO_4, thus retained at the batteries and not released during the heating cycle.

Due to reactions 29 and 65, as well as others between SO_x, HCl and either manganese oxides or zinc oxides, for example, reactions 31 and 32 (and others not referred to in (Appendix), the components of alkaline batteries must be considered useful reactants for cleaning the acid gases produced at the MSW incinerators. About 80% of the sulfur emitted during the combustion of alkaline batteries is collected as condensate salts in the zones of the off-gas treatment system above 470 K, meaning a high acid neutralizing potential of some of the components in the batteries. This aspect must be taken into account to carry out the life cycle analysis of batteries at the incineration disposal process, since it means that less neutralizing alkaline reagent is needed for the cleaning gas treatment.

4. Conclusions

The incineration of spent alkaline batteries at MSW incinerator plants is not generally considered an appropriate method of disposal for this residue, since it wastes recyclable materials and it is a source of gaseous emissions that must be cleaned by the off-gas treatment systems. Mercury, the most volatile trace element in alkaline batteries, as well as mercury (II) chloride resulting from chloridizing reactions with HCl produced in the combustion of chlorinated materials, like PVC plastics, both increase the gas cleaning difficulties experienced at the MSW incineration plants. Mercury released from batteries will contribute generally with a reduced amount of the metal that must be captured by the incinerator cleaning system.

Although HCl is usually formed when chlorinated materials burn, most of the HCl from the PVC plastic sleeve combustion combines with KOH and metals in the batteries to form salts with lower volatility than HCl. It is expected that about 36% of chlorides resulting from the combustion of alkaline batteries in MSW incinerators are as condensates on the fly ashes collected by the off-gas treatment system; the remaining chlorides, representing more than 60% of chlorine in the PVC plastic sleeve, enter the composition of bottom ashes in the form of very stable metallic chlorides, for example, KCl.

Zinc is with no doubt the most emitted metal from spent batteries due to vaporization of metal still present in the anode, its oxidation to ZnO and subsequent particles formation. Most of the zinc in the alkaline batteries fed to a MSW incinerator will be found in the bottom ashes, except that in small particles of ZnO that are carried on the gases by a mechanical carrying action. A small portion in the form of zinc chloride obtained by the thermodynamically feasible combinations of HCl with both the metal and ZnO (either in the anode or from anodic zinc vaporization and oxidation) can use the fly ashes as a nucleus for its condensation, therefore it is transportable far way from the furnace. Although the experimental tests indicate 6.5% of Zn in batteries as zinc emissions, this percentage is strongly dependent on the use of batteries, since it influences the relative percentages of zinc metal and zinc oxide in the anode material at the moment of incineration. Furthermore, MSW fed into an incinerator furnace generates HCl from a large spectrum of other chlorinated materials usually present in its composition, namely PVC materials, therefore influence the intensity of chloridizing reactions producing $ZnCl_2$ and its percentage in the fly ashes.

Manganese, another abundant metal in batteries as oxide, gives no appreciable gaseous emissions and practically all of it will be found in the MSW incinerator bottom ashes as oxide. Traces of manganese chlorides can be found in the fly ashes as a result of the reactions between HCl and manganese oxides present in the cathode of batteries.

Practically, all iron from the outside steel can of the alkaline batteries will be recovered with other iron scrap in the bottom ashes through a magnetic selection procedure typically used in the MSW incinerating plants. However, much of the iron in the steel cans will be strongly oxidized in the burning process originating a less valuable iron scrap. Only a low amount of iron can be chloridized and the respective iron chloride further condensates on the fly ashes.

Fly ashes may also have traces of lead, copper and other less volatile metals in the batteries, mainly due to chloridizing reactions with HCl that form their volatile chlorides; mechanical carrying actions of small ash particles from the burning process of combustible materials containing the metals as impurities, pigments or fillers can add negligible amounts of those metals to the composition of fly ashes.

The presence of chromium in the MSW incinerator fly ashes due to the incineration of batteries is improbable, since it may have found some thermodynamic support only in the oxidizing reactions to the less frequent Cr(VI) and Cr(IV).

KOH from the batteries' electrolyte can be vaporized at the temperatures found at the MSW incinerator furnace operation. Some of it, after condensation, can participate in unwanted reactions with materials of the furnace grate, furnace liner materials and boiler walls, therefore shortening useful life cycle of these components.

Despite this possibility, KOH, as well as zinc metal and in a less amount both zinc and manganese oxides in the anode and cathode have the role of neutralizing agents of HCl and SO_x gases. KOH, too, combines with CO_2 very easily, and thus contributes to decrease greenhouse impact of the incineration process. These positive actions of the alkaline batteries in the incineration process must be balanced with the other effects when one wants to assess advantages and disadvantages of this disposal process, namely through life cycle analysis.

Acknowledgement

The authors acknowledge the financial support from Fundação para a Ciência e a Tecnologia, under the research project POCTI/1999/CTA/35616.

Appendix A

When an alkaline battery is heated at 1200–1300 K under oxidant atmosphere, most of the reactions among its components, as well as between them and the gases, may be anticipated through thermodynamic data (Knacke et al., 1991). The purpose of this appendix is to use some of the thermodynamic information to help to explain emissions of batteries on the experimental tests carried out, as well as at the MSW incineration process.

A.1. PVC

PVC from the batteries sleeve is a chlorinated hydrocarbon with chloride content in the range of 55–60% of dry mass or above. PVC is never used alone, but always mixed with heat stabilizers, lubricants, plasticizers, fillers, and other additives to make processing possible (Ullmann's Encyclopedia of Industrial Chemistry, 2002).

Combustion of chlorinated hydrocarbons can be described by Eq. (1) (Vovelle, 2000):

$$C_xH_yCl_z + xO_2 \rightarrow xCO_2 + zHCl + (y - z)/2H_2O. \quad (1)$$

For $y > z$, as in the case of PVC, the thermodynamically preferred combustion chlorinated product is HCl. Combustion of chlorinated compounds may be associated with the formation of potentially toxic byproducts. These byproducts include chlorinated alkenes as well as chlorinated aromatics, chlorinated dioxins and furans (Vovelle, 2000).

A.2. Polyamide

Polyamide, on the plastic grommet of batteries, is a family of polymerized hydrocarbons with methylene groups and carbonamide groups with nitrogen, where C and H content depend on the monomer starting material (Ullmann's Encyclopedia of Industrial Chemistry, 2002). Therefore, polyamide combustion will generate CO_2, H_2O, N_2 and some NO_x, particularly NO, whose amount is strongly dependent on the so-called fuel nitrogen that is nitrogen chemically bound in the fuel. The extent of fuel nitrogen conversion to NO_x is nearly independent of molecular structure, but strongly dependent on the level of nitrogen compounds in the fuel and on the local combustion conditions, i.e., stoichiometry and temperature (Vovelle, 2000). The thermal and prompt mechanisms of NO formation will have a reduced importance in the formation of NO_x in polyamide combustion. From the point of view of NO formation, the level of temperature in MSW incinerator furnace is low, and in the low-pressure flames, NO levels due to prompt formation mechanisms are typically less than 1 ppm (Vovelle, 2000).

A.3. Coal and paper

Graphitic carbon on the cathode, as well as other from cardboard, paper and cellophane, will burn according to reaction 25 (Table A.1). Under reducing conditions carbon dioxide may react with carbon to generate CO following the well-known Boudouard reaction $C + CO_2 \rightarrow 2CO$ whose ΔG° is about -38.7 and -56.1 kJ, respectively at 1200 and 1300 K (Coudurier and Hopkins, 1985). Despite these values, the rate of this reaction is not very important at these temperatures. Hydrogen in hydrocarbons will burn, producing water as in reaction 26 (Table A.1).

A.4. Zinc

Even at temperatures below its boiling point, zinc vapor pressure is already very important, as may be seen through equation $p_{Zn} = -6.85/T \ -1.255 \log T + 9.46$ (Darcy, 1986). So, metallic

Table A.1
Oxidation reactions with elements in the alkaline AA Duracell® batteries[a]

No.	Reaction	$\Delta G^{\circ}_{1200\ K}$	$\Delta G^{\circ}_{1300\ K}$	m.p., K	B.p., K	m.p., K
1	$Zn + 1/2\ O_2 \rightarrow ZnO$	−224.8	−204.4	693	1179	2243
2	$2MnO_2 \rightarrow Mn_2O_3 + 1/2O_2$	[b]	[b]	803	Decomp.	1361
3	$3Mn_2O_3 \rightarrow 2Mn_3O_4 + 1/2O_2$	11.7	4.4	1361	Decomp.	1835
4	$3Mn_2O_3 + CO \rightarrow 2Mn_3O_4 + CO_2$	−167.3	−166.1	1361	Decomp.	1835
5	$3Mn_2O_3 + C \rightarrow 2Mn_3O_4 + CO$	−206.6	−222.6	1361	Decomp.	1835
6	$Mn_2O_3 + 3CO \rightarrow 2Mn + 3CO_2$	113.4	113.6	1361	Decomp.	2083
7	$Mn_3O_4 + 4CO \rightarrow 3Mn + 4CO_2$	253.7	253.4	1835	Decomp.	2083
8	$Mn_3O_4 + 4C \rightarrow 3Mn + 4CO$	96.6	27.2	1835	Decomp.	2083
9	$2Fe + 3/2O_2 \rightarrow Fe_2O_3$	−510.5	−485.7	1809	3158	1730
10	$Sn + O_2 \rightarrow SnO_2$	−331.7	−311.4	505	2873	1893
11	$Cu + 1/2\ O_2 \rightarrow CuO$	−49.8	−41.6	1358	2842	1364
12	$2Cu + 1/2\ O_2 \rightarrow Cu_2O$	−81.0	−73.8	1358	2842	1517
13	$Ni + 1/2\ O_2 \rightarrow NiO$	−132.2	−123.8	1728	3169	2228
14	$Pb + 1/2\ O_2 \rightarrow PbO$	−100.7	−93.5	601	2020	1897
15	$2Cr + 3/2O_2 \rightarrow Cr_2O_3$	−825.5	−800.3	2130	2952	2603
16	$Cr + 3/2O_2 \rightarrow CrO_3$	−210.8	−203.5	2130	2952	470
17	$Cr + 1/2\ O_2 \rightarrow CrO$	58.8	48.9	2130	2952	[c]
18	$Cr + O_2 \rightarrow CrO_2$	−117.6	−120.3	2130	2952	[c]
19	$Co + 1/2\ O_2 \rightarrow CoO$	−149.4	−142.5	1768	3200	2103
20	$Cd + 1/2\ O_2 \rightarrow CdO$	−121.2	−101.6	594	1039	1755
21	$As_4 + 3O_2 \rightarrow As_4O_6$	−731.1	−682.4	1090[d]	875	582[e]
22	$2Sb + 2O_2 \rightarrow Sb_2O_4$	−452.6	−412.6	904	1858	1524
23	$4Sb + 3O_2 \rightarrow Sb_4O_6$	−770.2	−726.8	904	1858	928
24	$2Tl + 1/2O_2 \rightarrow Tl_2O$	−78.7	−78.2	577	1744	852[f]
25	$C + O_2 \rightarrow CO_2$	−397.3	−397.5	–	4055	216.4[g]
26	$H_2 + 1/2\ O_2 \rightarrow H_2O$	−182.0	−176.4	15.9	20.4	273
27	$4KOH + Cr_2O_3 + 3/2O_2 \rightarrow 2\ K_2CrO_4$	−432.8	−426.4	679	1589	1250
	$+2H_2O$			2603	–	273
28	$2KOH + CO_2 \rightarrow K_2CO_3 + H_2O$	−72.7	−65.8	679	1589	1173
29	$2KOH + SO_3 \rightarrow K_2SO_4 + H_2O$	−333.6	−322.7	679	1589	1342[h]

[a] Melting point (m.p.) and boiling point (b.p.) of reactants in columns 5 and 6; m.p. of main reaction product in column 7.
[b] Decomposes to Mn_2O_3 at 803 K.
[c] Vapor in equilibrium with Cr_2O_3.
[d] At 4140 kPa.
[e] B.p. 670 K.
[f] B.p., 1257 K.
[g] At 500 kPa; b.p. 194.7.
[h] Decomposes at 2379 K.

powdered zinc in the anode will be vaporized and carried on as one of the gaseous components in the off-gas stream. However, as zinc is a very reactive element, it combines with oxygen according to reaction 1 (Table A.1) to produce zinc oxide. Since this compound is solid at temperatures below 2248 K (Coudurier and Hopkins, 1985), zinc in the off-gases transforms into fine particles of zinc oxide.

ZnO in the anode stays as such at the experimental furnace refractory steel tube and at the furnace grate of MSW incinerator, in this case incorporating bottom ashes. However, ZnO may also participate in reactions with other components in batteries or in MSW. Reactions 30 and 31 (Table A.2) produce $ZnCl_2$ that is more volatile than Zn, and, consequently, is carried on the gases. These chloridization reactions with HCl or other chlorides are more probable than chlorination reactions with Cl_2 generated through hydrogen deficient processes of combustion or the known Deacon reaction: $2HCl + 1/2O_2 \rightarrow Cl_2 + H_2O$ favored by excess of air and low temperatures (Vovelle, 2000). Zinc may participate in other reactions at the incinerator and some of them can contribute to the cleaning gas process.

A.5. KOH

KOH has melting and boiling points, respectively, at 683 and 1600 K (Ullmann's Encyclopedia of Industrial Chemistry, 2002). This compound has partial vapor pressure of 2.58 and 8.28 kPa at 1200 and 1300 K, respectively (Knacke et al., 1991). Such pressure is of the same order of magnitude of water vapor at about 295 and 315 K (Sinnot, 1993). Thus, KOH can be evaporated in some extension reacting with other substances, namely those present in the off-gas flow. Reaction 28 (Table A.1) with CO_2 is foreseen, since carbon dioxide is an abundant component on the combustion process of organic matter and hydrocarbons. Reaction 29 (Table A.1) with sulfur oxide and reaction 65 (Table A.2) with chloridric acid both contribute to fix these pollutants in very stable compounds. Reaction 27 (Table A.1) with chromium sesquioxide is the basis of potassium chromate production, a very soluble specie of Cr(VI).

A.6. Manganese

In the alkaline batteries cathode exist simultaneously the main initial manganese oxide MnO_2 as well as Mn_3O_4, as a result of manganese dioxide transformation through the electrochemical reaction to produce electricity. The first oxide is stable until 770 K, Mn_2O_3 up to 1250 K and Mn_3O_4 until 1900 K (Atimtay and Harrison, 1998). So, on heating batteries, the natural tendency is MnO_2 to be changed into Mn_2O_3, at 770 K, according to reaction 2 (Table A.1) and, following, into Mn_3O_4,above 1250 K, according to reaction 3 (Table A.1). The graphite present in the cathode may increase the rate of such transformations both as C and as CO. In the first case, a close contact between the two solid reagents must be achieved in order to make possible the reduction reaction; in the second reaction, since CO is a gas, the contact between it and manganese oxide has better conditions to occur. Thus, reactions 4, 5, 6, 7 and 8 (Table A.1) can be considered for manganese oxides in the cathode. Therefore, almost all the manganese is on the cathode as Mn_3O_4 at 1200–1300 K or as other manganese compounds resulting from reactions with components in the MSW or gener-

Table A.2
Chloridizing reactions and other reactions with elements in alkaline AA Duracell® batteries[a]

No.	Reaction	$\Delta G^\circ_{1200\ K}$	$\Delta G^\circ_{1300\ K}$	m.p., K	B.p., K
30	$Zn + 2HCl + 1/2O_2 \rightarrow ZnCl_2 + H_2O$	−249.6	−232.7	591	1004
31	$ZnO + 2HCl \rightarrow ZnCl_2 + H_2O$	−24.9	−28.3	591	1004
32	$Mn_3O_4 + 6HCl + CO \rightarrow 3MnCl_2 + 3H_2O + CO_2$	−158.4	−140.9	924	1509
33	$Fe + 2HCl + 1/2O_2 \rightarrow FeCl_2 + H_2O$	−183.6	−169.0	950	1293
34	$Fe + 3HCl + 3/4O_2 \rightarrow FeCl_3 + 3/2H_2O$	−196.5	−183.5	577	604
35	$Fe_2O_3 + 6HCl \rightarrow 2FeCl_3 + 3H_2O$	117.4	118.7	577	604
36	$Fe_2O_3 + 4HCl + CO \rightarrow 2FeCl_2 + 2H_2O + CO_2$	−35.8	−22.7	950	1293
37	$Ni + 2HCl + 1/2O_2 \rightarrow NiCl_2 + H_2O$	−106.5	−99.0	1304[b]	1228
38	$NiO + 2HCl \rightarrow NiCl_2 + H_2O$	25.7	24.8	1304[b]	1228
39	$Cr + 3HCl + 3/4O_2 \rightarrow CrCl_3 + 3/2H_2O$	−244.2	−230.1	1088	1279
40	$Cr_2O_3 + 6HCl \rightarrow 2CrCl_3 + 3H_2O$	337.0	340.0	1088	1279
41	$Cr_2O_3 + 4HCl + CO \rightarrow 2CrCl_2 + 2H_2O + CO_2$	185.1	195.2	1088	1576
42	$CrO_3 + 2HCl \rightarrow CrOCl_2 + H_2O$	−159.4	−147.8	[c]	390
43	$Cu + HCl + 1/4O_2 \rightarrow CuCl + 1/2H_2O$	−3.2	−8.0	709	1482
44	$Cu + 2HCl + 1/2O_2 \rightarrow CuCl_2 + H_2O$	–	–	683[d]	–
45	$Cu_2O + 2HCl \rightarrow 2CuCl + H_2O$	74.5	57.9	709	1482
46	$CuO + 2HCl \rightarrow CuCl_2 + H_2O$	–	–	683[d]	–
47	$Sn + 2HCl + 1/2O_2 \rightarrow SnCl_2 + H_2O$	−198.0	−191.9	520	885
48	$SnO_2 + 4HCl \rightarrow SnCl_4 + 2H_2O$	70.2	77.5	240	382
49	$SnO_2 + 2HCl + CO \rightarrow SnCl_2 + CO_2 + H_2O$	−45.4	−51.1	520	885
50	$PbO + 2HCl \rightarrow PbCl_2 + H_2O$	−78.3	−77.5	774	1223
51	$Pb + 2HCl + 1/2O_2 \rightarrow PbCl_2 + H_2O$	−179.1	−170.9	774	1223
52	$Co + 2HCl + 1/2O_2 \rightarrow CoCl_2 + H_2O$	−141.3	−127.2	994	1354
53	$Co + 3HCl + 3/4O_2 \rightarrow CoCl_3 + 3/2H_2O$	−93.3	−79.7	[e]	–
54	$CoO + 2HCl \rightarrow CoCl_2 + H_2O$	8.2	15.3	994	1354
55	$CoO + 3HCl + 1/2\ O_2 \rightarrow CoCl_3 + H_2O$	371.9	397.0	[e]	–
56	$Cd + 2HCl + 1/2O_2 \rightarrow CdCl_2 + H_2O$	−683.0	−688.1	842	1236
57	$CdO + 2HCl \rightarrow CdCl_2 + H_2O$	−65.3	−65.7	842	1236
58	$Tl + HCl + 1/4O_2 \rightarrow TlCl + 1/2H_2O$	−73.0	−69.2	704	1083
59	$Tl_2O + 2HCl \rightarrow 2TlCl + H_2O$	−202.5	−207.8	704	1083
60	$Sb + 3HCl + 3/4O_2 \rightarrow SbCl_3 + 3/2H_2O$	−902.5	−932.0	346	496
61	$Sb_4O_6 + 12HCl \rightarrow 4SbCl_3 + 6H_2O$	−125.6	−102.7	346	496
62	$As_4 + 12HCl + 3O_2 \rightarrow 4AsCl_3 + 6H_2O$	−652.7	−580.0	263	403
63	$As_4O_6 + 12HCl \rightarrow 4AsCl_3 + 6H_2O$	78.4	102.4	263	403
64	$Hg + 2HCl + 1/2O_2 \rightarrow HgCl_2 + H_2O$	−61.6	−45.1	550	576
65	$KOH + HCl \rightarrow KCl + H_2O$	−146.4	−145.3	1045	1714

[a] Melting point and boiling point of main product at columns 5 and 6.
[b] Decomposes.
[c] Known as gas.
[d] Decomposes into $CuCl + Cl_2$.
[e] Known as gas.

ated at the batteries themselves. One of them is reaction 32 (Table A.2), which generates $MnCl_2$, with a vapor pressure of 4.35 kPa at 1200 K.

A.7. Iron

Steel components, most of it iron, are oxidized through reaction 9 (Table A.1). An experiment with a steel can heated at 1273 K for 1 h gave a mass increase of 42.5%, meaning a high rate of the oxidation process. Iron sesquioxide cannot be chloridized in oxidant atmospheres as indicated by reaction 35 (Table A.2). On the contrary, in a reducing atmosphere, the production of $FeCl_2$ is possible, as reaction 36 (Table A.2) indicates. The direct chloridization of iron is possible both to produce $FeCl_2$ and $FeCl_3$, although this last is favored due to the higher volatility of the iron compound formed, as seen in reactions 33 and 34 (Table A.2).

A.8. Copper and tin

Yellow brass is a well-known copper alloy with about 60% Cu that melts around 1198 K. Tin on the surface of the tin-plated brass anode collector melts at 505 K and tin is a traditional alloying element in copper alloys, therefore relatively miscible with it. According to reaction 10 (Table A.1), tin not incorporated into brass will be transformed into SnO_2. This oxide cannot be chloridized in oxidant atmospheres as demonstrated by reaction 48 (Table A.2). The same does not occur in reducing atmospheres, as shown by reaction 49 (Table A.2), which produces Sn(II) chloride. Direct chloridization of tin is possible in oxidant atmospheres as indicated by reaction 47 (Table A.2). Copper may also be oxidized through reactions 11 and 12 (Table A.1), the second being more feasible than the first, which forms cupric oxide. This oxide decomposes into cuprous oxide at the 1200–1300 K range of temperature. Copper oxides chloridization through reactions 45 and 46 (Table A.2) is not thermodynamically feasible. For the latter, thermodynamic data were not found to calculate the respective ΔG° in the range of 1200–1300 K, since $CuCl_2$ decomposes into CuCl and Cl_2. Direct chloridization of copper is possible, as demonstrated in reaction 43. Near the surface of the brass, a small part of zinc carrying out some copper will be lost by vaporization and oxidized on the gas or on the surface of melted brass. This fuming phenomenon is well known at non-ferrous foundries.

A.9. Nickel

Nickel metal present in the batteries is oxidized to NiO, according to reaction 13 (Table A.1). This oxide is not chloridizable as shown in reaction 38 (Table A.2). On the contrary, reaction 37 shows that nickel metal can be directly chloridized under oxidant conditions.

A.10. Lead

Lead will be oxidized following reaction 14 (Table A.1), and this oxide may be chloridized through reaction 50 (Table A.2), as well as the lead metal, as shown in reaction 51.

A.11. Chromium

Chromium on the surface of steel components may have the four oxidation possibilities given by reactions 15, 16, 17 and 18 (Table A.1). Cr_2O_3 production is by far the most feasible, followed by CrO_3 and then by CrO_2. The latter two oxides are gases at 1200 and 1300 K, contrary to the first that melts only at 2603 K. Chloridization of chromium oxides is only possible to produce chromyl chloride, as indicated by reaction 42, since reactions 40 and 41 (Table A.2) are not thermodynamically feasible. Chromium also can be directly chloridized, as seen in reaction 39.

A.12. Cobalt

Cobalt in steels may be oxidized through reaction 19 (Table A.1) and chloridized through reaction 53. Chloridization of the oxide is not feasible either to produce $CoCl_2$ or $CoCl_3$. This latter chloride is not known as a solid compound, but only in the gaseous state.

A.13. Cadmium

Cadmium, known as a normal impurity present in zinc, coming from its primary raw sulfide materials, is also present in the batteries as trace. It may suffer oxidation through reaction 20 (Table A.1). As Cd boiling point is 1039 K, a certain amount of it will be oxidized on the gas flow after vaporization. Cadmium chloride may be produced from both Cd and CdO, as indicated by reactions 56 and 57 (Table A.2).

A.14. Arsenium

As_4O_6 gas can be produced similarly to reaction 21 (Table A.1) from the As_4, As_3, As_2 and As species in the gas at 1200 and 1300 K, in which the first is predominant. Chloridization of arsenium may be done directly from the metal, as seen in reaction 62 (Table A.2), since As_4O_6 is more stable than As(III) chloride in oxidant atmospheres.

A.15. Antimonium

Antimonium may be oxidized through reactions 22 and 23 (Table A.1), the second producing a gaseous compound at 1200 and 1300 K. Even Sb_2O_4 has a non-negligible vapor pressure of 0.11 and 1.06 kPa, respectively, at those temperatures. Antimonium may be chloridized both directly as metal and Sb_4O_6, according to reactions 60 and 61 (Table A.2).

A.16. Thalium

Vapor pressure of thalium is 0.55 and 2.01 kPa at 1200 and 1300 K, respectively. Reaction 24 (Table A.1) with oxygen produces Tl_2O whose boiling point is 1257 K. Thus, thalium may be released into the gases as oxide or metal that is further oxidized. Thalium chloride may be obtained through reactions 58 and 59 (Table A.2).

A.17. Mercury

Mercury is a highly volatile metal whose boiling point is 629 K. Its oxide is unstable and decomposes at temperatures below 1200 K. Mercury (II) chloride is obtainable through reaction 64 (Table A.2), and it is more volatile than the metal form. The Hg_2Cl_2 chloride, whose melting point is 655 K, decomposes into Hg and $HgCl_2$, the only stable chloride at higher temperatures. High volatile organic compounds of mercury, such methyl mercury can be formed under reducing conditions.

A.18. Sulfur

Sulfur in oxidant atmospheres may be present as SO_3, SO_2, SO and S_2O, the first two being the dominant species. From a thermodynamic point of view, SO_3 is the most favorable sulfur oxide at temperatures below 1073 K. Thus, SO_2 is the predominant oxide in the range of 1200–1300 K. Other species may also exist under reducing conditions, as, for example, CS_2 and COS.

References

Almeida, M.F., Xará, S.M., Delgado, J., Costa, C.A., 2006. Characterization of spent AA household alkaline batteries. Waste Management 26, 466–476.

American Public Health Association, American Water Works Association & Water Environmental Federation, 1992. Standard Methods for The Examination of Water and Wastewater. Gravimetric Method with Ignition of Residue. 4500 – SO_4^{2-} C., Washington, DC, US.

Atimtay, A.T., Harrison, D.P., 1998. Desulfurization of Hot Coal Gas. NATO ASI Series, Series G: Ecological Sciences, vol. 42. Springer-Verlag.

Bassett, J., Denny, R., Jeffery G., Mendham, J., 1981. Análise inorgânica quantitativa (Quantitative Inorganic Analysis), Editora Guanabara, S.A., Rio de Janeiro.

Coudurier, L., Hopkins, D.W., 1985. Fundamentals of Metallurgical Processes, second ed. Pergamon Press.

Darcy, M., 1986. Métallurgie du Zinc. Techniques de l'Ingénieur, Paris.

European Parliament and Council, Directive 2000/76/EC on the incineration of waste, 2000. OJ L 332, p. 91.

Knacke, O., Kubaschewski, O., Hesselmann, K., 1991. Thermochemical Properties of Inorganic Substances. Springer-Verlag.

Labouze, E., Monier, V., 2003. Impact Assessment on Selected Policy Options for Revision of the Battery Directive, BIO Intelligence Service.

Sinnot, R.K., 1993, second ed. Coulson & Richardson's Chemical Engineering, vol. 6 Pergamon Press.

Ullmann's Encyclopedia of Industrial Chemistry, 2002. 6th ed., electronic edition.

United States Environmental Protection Agency (USEPA), 1982. Test methods for evaluating solid waste, physical/chemical methods SW846. Method 7000A – Atomic Absorption Methods, second ed. Office of Solid Waste and Emergency Response, Washington, DC.

Vovelle, C., 2000. Pollutants from Combustion. Formation and Impact on Atmospheric Chemistry. NATO Science Series, Series C: Mathematical and Physical Sciences, vol. 547. Kluwer Academic Publishers.